Observer design for a class of uncertain nonlinear systems with sampled outputs - Application to the estimation of kinetic rates in bioreactors

Ibtissem Bouraoui, Mondher Farza, Tomas Ménard, Ridha Ben Abdennour, Mohammed M'Saad, Henda Mosrati

Observer design for a class of uncertain nonlinear systems with sampled outputs - Application to the estimation of kinetic rates in bioreactors

I. Bouraoui [a,b], M. Farza [a], T. Ménard [a] R. Ben Abdennour [b] M. M'Saad [a]
H. Mosrati [c]

[a] *GREYC, UMR 6072 CNRS, Université de Caen, ENSICAEN, 6 Bd Maréchal Juin, 14050 Caen, France*

[b] *Unité de Recherche CONPRI, ENIG Gabès, Rue Omar Ibn El Khattab, 6029 Gabès, Tunisie*

[c] *UR ABTE, EA 4651, Université de Caen, Bd Maréchal Juin, 14032 Caen, France*

Abstract

A continuous-discrete time observer is proposed for a class of uncertain nonlinear systems where the output is available only at non uniformly spaced sampling instants. The underlying correction term depends on the output observation error and is updated in a mixed continuous-discrete fashion. The proposed observer is first introduced under a set of differential equations with instantaneous state impulses corresponding to the measured samples and their estimates. Two features of the proposed observer are worth to be pointed out. The first one consists in the simplicity of its calibration while the second one lies in its comprehensive convergence analysis. More specifically, it is shown that in the case of noise-free sampled outputs, the observation error lies in a ball centered at the origin and which radius is proportional to the bounds of the uncertainties and the sampling partition diameter. Moreover, in the free uncertainties case, the exponential convergence to zero of the observation error is established under a well-defined condition on the maximum value of the sampling partition diameter. The ability of the proposed observer to perform a suitable estimation of the reactions rates in biochemical reactors is highlighted through a simulation study dealing with an ethanolic fermentation.

Key words: Nonlinear systems, high gain observers, impulsive systems, continuous-discrete time observers, bioreactors, reactions rates.

1 Introduction

Although a considerable research activity has been devoted to the observer design for nonlinear systems over the last decades, the available contributions deal mainly with the continuous-time measurements case [14, 19, 12, 1, 25, 21]. In order to handle the non continuous availability of the output measurements, many works have focused on the redesign of the continuous time state observers that have been proposed for the underlying systems. An early contribution was made using a high gain observer for a class of nonlinear systems that are observable for any input [7]. The design was firstly carried out assuming continuous-time output measurements before being appropriately modified to deal with the case where these measurements are only available at sampling instants. Based on the aforementioned contribution, many other observers have been proposed for specific classes of continuous time systems with sampled output measurements [16, 22]. In all these contributions, the continuous-discrete time observer operates as follows: a dynamical system, which is similar to the underlying system, is used to provide a state prediction over the sampling intervals. At the sampling instants, the output measurements are used to update the state prediction provided by the dynamical system. An output predictor approach has been proposed in [18] to cope with the non-availability of the output measurements between the sampling instants. It consists in a continuous time observer involving a suitable predictor of the output over the sampling intervals. More specifically, the output prediction is provided by the solution of an ordinary differential equation between two successive sampling instants with the value of the measured output sample as initial condition. The underlying observer is a hybrid system which is able to recover the continuous time observer properties for relatively fast sampling. Another approach was described in [24] where the authors proposed an impulsive continuous-discrete time observer for a class of uniformly observable systems with sampled outputs. The correction term of the pro-

Email address: `mondher.farza@unicaen.fr` (M. Farza).

posed observer is the product of a constant gain by the difference between the estimated and measured values of the last output sample. The determination of the observer gain is carried out through the resolution of an appropriate LMI.

In this paper, our objective consists in synthesizing a continuous-discrete time observer for a class of uncertain nonlinear systems where the output measurements are available only at non uniformly spaced sampling instants. In the absence of uncertainties, the considered class of nonlinear systems is observable for any input and has been considered in [11] for observer design purposes in the case where the output measurements are available in a continuous manner. The proposed continuous-discrete time observer is issued from a redesigned version of the high gain continuous time observer proposed in [11]. This observer shares the impulsive nature of the observer given in [24] up to an adequate modification of the observer gain matrix. Indeed, unlike in [24], the gain of the proposed observer does not necessitate the resolution of any system and its expression is given. This gain is time-varying and depends on the sampling periods. There are two main features of the proposed continuous-discrete time observer that are worth to be emphasized with respect to the existing ones. The first one concerns the ease with which the observer gain is updated at sampling instants together with the simplicity of its implementation. The second feature is related to the convergence analysis simplicity and its ability to provide precise expressions of the upper bounds of the sampling partition diameter as well as the rate of the observation error convergence. More specifically, it is shown that the observation error lies in a ball centered at the origin with a radius proportional to the magnitude of the bounds of the uncertainties, the noise measurements and the maximum sampling partition diameter. Moreover, it is shown that in the noise-free outputs case, the ultimate bound of the observation error can be made arbitrarily small, as in the continuous-time output case, when the maximum sampling partition diameter tends to zero. A particular emphasis is put on the fact that the observation error converges exponentially to the origin in the absence of uncertainties and noise measurements. Of particular interest, the expression of the underlying decay rate is given.

The paper is organized as follows. In the next section, the class of systems under consideration and the notations employed throughout this paper are introduced together with concise convergence results on the continuous time high gain observer on which the proposed continuous-discrete time observer is based upon. The output noise measurements are taken into account in the provided convergence analysis. A technical lemma with its proof are also given in this section and this lemma is used to establish the main result of the paper. Section 3 is devoted to the main contribution of the paper, namely the design of the continuous-discrete time observer. The fundamental result is given with a comprehensive proof thanks to the technical lemma derived in Section 2. In Section 4, the effectiveness of the proposed observer is highlighted via simulation results involving the estimation of the reactions rates in a bioreactor involving an ethanolic fermentation. Finally, some concluding remarks are given in Section 5.

Throughout the paper, I_p and 0_p will denote the p-dimensional identity and zero matrices respectively and $\|\cdot\|$ denotes the euclidian norm; λ_M (resp. λ_m) is the maximum (resp. minimum) eigenvalue of a certain Symmetric Positive Definite (SPD) matrix P and $\sigma = \sqrt{\lambda_M/\lambda_m}$ is its conditioning number.

2 Problem statement and preliminaries

Consider the class of multivariable nonlinear systems that are diffeomorphic to the following bloc triangular form:

$$\begin{cases} \dot{x}(t) = Ax(t) + \varphi(u(t), x(t)) + B\varepsilon(t) \\ y(t_k) = Cx(t_k) + w(t_k) = x^1(t_k) + w(t_k) \end{cases} \tag{1}$$

with

$$x = \begin{pmatrix} x^1 \\ \vdots \\ x^{q-1} \\ x^q \end{pmatrix} \in \mathbb{R}^n, \quad \varphi(u,x) = \begin{pmatrix} \varphi^1(u,x^1) \\ \varphi^2(u,x^1,x^2) \\ \vdots \\ \varphi^{q-1}(u,x^1,\dots,x^{q-1}) \\ \varphi^q(u,x) \end{pmatrix}$$

$$A = \begin{pmatrix} 0_{(q-1)p,p} & I_{(q-1)p} \\ 0_{p,p} & 0_{p,(q-1)p} \end{pmatrix}, \; B = \begin{pmatrix} I_p & 0_p & \dots & 0_p \end{pmatrix}^T,$$
$$C = \begin{pmatrix} I_p & 0_p & \dots & 0_p \end{pmatrix} \tag{2}$$

where $x^i \in \mathbb{R}^p$ for $i \in [1,\ q]$ are the state variables blocks, $u(t) \in U$ a compact subset of $\mathbb{R}^m$ denotes the system input and $y \in \mathbb{R}^p$ denotes the system output which is available only at the sampling instants that satisfy $0 \le t_0 < \dots < t_k < t_{k+1} < \dots$ with time-varying sampling intervals $\tau_k = t_{k+1} - t_k$ and $\lim_{k\to\infty} t_k = +\infty$; $w(t)$ is the output noise and $\varepsilon : \mathbb{R}^+ \mapsto \mathbb{R}^p$ is an unknown function describing the system uncertainties and may depend on the state, the input and uncertain parameters.

As it is mentioned in the introduction, our main objective is to design a continuous-discrete time observer providing a continuous time estimation of the full state of system (1) by using the output measurements that are available only at the sampling instants. Such a design will be carried out under the following assumptions :

A1. The state $x(t)$ is bounded i.e. there exists a compact set $\Omega \in \mathbb{R}^n$ such that $\forall t \ge 0,\ x(t) \in \Omega$.

A2. The functions φ^i for $i \in [1,\ q]$ are Lipschitz with respect to x uniformly in u, i.e.

$$\forall \rho > 0;\ \exists L > 0;\ \forall u\ s.t.\ \|u\| \le \rho; \forall (x,\bar{x}) \in \Omega \times \Omega : \\ \|\varphi^i(u,x) - \varphi^i(u,\bar{x})\| \le L\|x - \bar{x}\| \tag{3}$$

A3. The unknown function ε is essentially bounded, i.e. $\exists \delta_\varepsilon > 0$; $\sup_{t\ge 0} Ess\|\ \varepsilon(t)\| \le \delta_\varepsilon$

A4. The noise signal w is essentially bounded, i.e. $\exists \delta_w > 0$; $\sup_{t\ge 0} Ess\|w(t)\| \le \delta_w$

Furthermore, one naturally assumes that the time intervals τ_k's are bounded away from zero by τ_m and are upperly bounded by the upper bound of the sampling partition diameter τ_M, i.e.

$$0 < \tau_m \le \tau_k = t_{k+1} - t_k \le \tau_M, \quad \forall k \ge 0 \tag{4}$$

There are two remarks that are worth to be pointed out. Firstly, the class of systems described by (1) may seem very restrictive since it assumes a non prime dimension ($n = pq$) and the state blocks x^k have the same dimension p. This is not the case since it is shown in [15] that in the uncertainties-free case, system (1) is a normal form which characterizes a class of uniformly observable nonlinear systems that can be put under this form via an injective map (see e.g. [15, 10] for more details). Secondly, since the system state trajectory lies in a bounded set Ω, one can extend the nonlinearities $\varphi(u, x)$ in such a way that this extension becomes globally Lipschitz on the entire state space $\mathbb{R}^n$. The observer synthesis will then be based on the resulting extended system which coincides with the original system on the domain of interest i.e. Ω. One can refer to [26, 1] and references therein for more details on how to carry globally Lipschitz prolongations in the state observation context.

2.1 The underlying continuous-time high gain observer design

As mentioned above, the continuous-discrete time impulsive observer we shall propose is issued from an appropriate redesign of a purely continuous-time high gain observer that has been proposed for system (1) in the case where the output measurements are available in a continuous manner i.e.

$$\begin{cases} \dot{x}(t) = Ax(t) + \varphi(u(t), x(t)) + B\varepsilon(t) \\ y(t) = Cx(t) + w(t) = x^1(t) + w(t) \end{cases} \tag{5}$$

We will particularly use a continuous-time observer similar to that proposed in

$$\dot{\hat{x}}(t) = A\hat{x}(t) + \varphi(u(t), \hat{x}(t)) - \theta\Delta_\theta^{-1}K(C\hat{x}(t) - y(t)) \tag{6}$$

with

$$\Delta_\theta = diag\left(I_p, 1/\theta I_p, \ldots, 1/\theta^{q-1} I_p\right) \tag{7}$$

where $\hat{x} \in \mathbb{R}^n$ denotes the state estimate, $K = (K^1 = k_1 I_p \ \ldots \ K^q = k_q I_p)^T$ where the k_i's, $i = 1, \ldots, q$ are chosen such that the matrix $\bar{A} \triangleq A - KC$ is Hurwitz and $\theta \geq 1$ is a scalar design parameter.
Before stating the results summarizing the main properties of observer (6), we recall that since the matrix $\bar{A} \triangleq A - KC$ is Hurwitz, there exist a $n \times n$ SPD matrix P and a positive real μ such that

$$P\bar{A} + \bar{A}^T P \leq -2\mu I_n \tag{8}$$

We now state the following result.

Theorem 2.1 *Consider system (5) subject to assumptions* **A1** *to* **A4** *together with the observer (6). Then,*

$$\forall \rho > 0; \exists \theta_0 > 0;\ \forall \theta \geq \theta_0;\ \forall u \ s.t.\ \|u\|_\infty \leq \rho;\ \forall \hat{x}(0) \in \mathbb{R}^n;\ \textit{we have}$$
$$\|\hat{x}(t) - x(t)\| \leq \sigma\theta^{q-1} e^{-\frac{\mu\theta}{2\lambda_M}t}\|\hat{x}(0) - x(0)\| + \frac{2\sigma\lambda_M}{\mu}\left(\frac{\delta_\varepsilon}{\theta} + \theta^{q-1}\|K\|\delta_w\right)$$

where x is the unknown system trajectory associated to the input u, $\hat{x}$ is any trajectory of the observer associated to (u, y), $\mu > 0$ is a positive real given by (8) and δ_ε and δ_w are the upper essential bounds of $\|\varepsilon(t)\|$ and $\|w(t)\|$, respectively with $\theta_0 = \max(1, 2L\sqrt{n}\lambda_M/\mu)$ and $\sigma = \sqrt{\lambda_M/\lambda_m}$ is the conditioning number of the matrix P given by (8).

The proof of the observation error convergence is similar to that given in [11] in the free noise output case. For clarity purposes and since the link between this observer and the continuous-discrete time one shall be raised, we shall detail the convergence analysis which accounts for the output noise measurements. Indeed, let $\tilde{x} = \hat{x} - x$ be the observation error. One has

$$\dot{\tilde{x}} = (A - \theta\Delta_\theta^{-1}KC)\tilde{x} + \varphi(u, \hat{x}) - \varphi(u, x) - B\varepsilon(t) + \theta\Delta_\theta^{-1}Kw(t)$$

Let $\bar{x} = \Delta_\theta\tilde{x}$. Taking into account the following identities

$$\Delta_\theta A\Delta_\theta^{-1} = \theta A \text{ and } C\Delta_\theta^{-1} = C \tag{9}$$

one gets

$$\dot{\bar{x}} = \theta\bar{A}\bar{x} + \Delta_\theta\left(\varphi(u, \hat{x}) - \varphi(u, x)\right) - \Delta_\theta B\varepsilon(t) + \theta Kw(t) \tag{10}$$

Let us show that $V(\bar{x}) = \bar{x}^T P\bar{x}$ is a Lyapunov function for system (10). Indeed, one has

$$\begin{aligned}\dot{V}(\bar{x}) \leq &-2\mu\theta\|\bar{x}\|^2 + 2\bar{x}^T P\Delta_\theta\left(\varphi(u, \hat{x}) - \varphi(u, x)\right) \\ &- 2\bar{x}^T P\Delta_\theta B\varepsilon(t) + \theta\bar{x}^T PKw(t)\end{aligned} \tag{11}$$

According to the Lipschitz assumption and the triangular structure of φ, one can show that for $\theta \geq 1$ [11, 15]:

$$2\bar{x}^T P\Delta_\theta\left(\varphi(u, \hat{x}) - \varphi(u, x)\right) \leq 2\sqrt{n}\lambda_M L\|\bar{x}\|^2 \tag{12}$$

where L is the Lipschitz constant of φ. Similarly, according to the structures of B and Δ_θ, one has

$$\begin{aligned}&2\bar{x}^T P\Delta_\theta B\varepsilon(t) \leq 2\frac{\|\varepsilon(t)\|\sqrt{\lambda_M}}{\theta^{q-1}}\sqrt{V(\bar{x})} \\ &2\theta\bar{x}^T PKw(t) \leq 2\theta\|w(t)\|\sqrt{\lambda_M}\|K\|\sqrt{V(\bar{x})}\end{aligned} \tag{13}$$

And combining (11), (12) and (13), one gets

$$\begin{aligned}\dot{V}(\bar{x}) \leq &-2(\mu\theta - \sqrt{n}\lambda_M L)\|\bar{x}\|^2 \\ &+ 2\sqrt{\lambda_M}\left(\|\varepsilon(t)\|/\theta^{q-1} + \theta\|K\|\|w(t)\|\right)\sqrt{V(\bar{x})}\end{aligned} \tag{14}$$

Choosing θ such that $2(\mu\theta - \sqrt{n}\lambda_M L) > \mu\theta$ i.e.

$$\theta > \theta_0' \triangleq 2L\sqrt{n}\lambda_M/\mu \tag{15}$$

Inequation (14) becomes

$$\dot{V}(\bar{x}) \leq -\frac{\mu\theta}{\lambda_M}V(\bar{x}) + 2\sqrt{\lambda_M}\left(\frac{\|\varepsilon(t)\|}{\theta^{q-1}} + \theta\|K\|\|w(t)\|\right)\sqrt{V(\bar{x})}$$

Or equivalently

$$\frac{d}{dt}\sqrt{V(\bar{x}(t))} \leq -\frac{\mu\theta}{2\lambda_M}\sqrt{V(\bar{x}(t))} + \sqrt{\lambda_M}\left(\frac{\|\varepsilon(t)\|}{\theta^{q-1}} + \theta\|K\|\|w(t)\|\right)$$

Using the comparison lemma [20], one gets

$$\sqrt{V(\bar{x}(t))} \leq \exp\left[-\frac{\mu\theta}{2\lambda_M}t\right]\sqrt{V(\bar{x}(0))} + \frac{2\lambda_M^{3/2}}{\mu\theta}\left(\frac{\delta_\varepsilon}{\theta^{q-1}} + \theta\|K\|\delta_w\right)$$

This yields to

$$\|\bar{x}(t)\| \leq \sigma\exp\left[-\frac{\mu\theta}{2\lambda_M}t\right]\|\bar{x}(0)\| + \frac{2\lambda_M\sigma}{\mu\theta}\left(\frac{\delta_\varepsilon}{\theta^{q-1}} + \theta\|K\|\delta_w\right) \tag{16}$$

Now, since $\bar{x} = \Delta_\theta\tilde{x}$, one has $\|\bar{x}(t)\| \leq \|\tilde{x}(t)\| \leq \theta^{q-1}\|\bar{x}(t)\|$ and inequation (16) leads to

$$\begin{aligned}\|\tilde{x}(t)\| \leq &\ \theta^{q-1}\sigma\exp\left[-\frac{\mu\theta}{2\lambda_M}t\right]\|\tilde{x}(0)\| \\ &+ \frac{2\lambda_M\sigma}{\mu}\left(\frac{\delta_\varepsilon}{\theta} + \theta^{q-1}\|K\|\delta_w\right)\end{aligned} \tag{17}$$

This ends the proof of theorem 2.1.
From (17), one can naturally conclude that in the noise free case, the proposed observer has the following properties: in the absence of uncertainties, i.e. $\delta_\varepsilon = 0$, the observation error converges exponentially to zero. If $\delta_\varepsilon \neq 0$

and is finite, the observation error lies in some ball centered at the origin with a radius proportional to δ_ε but it can be made arbitrarily small by choosing values of θ sufficiently high. However, high values of θ have to be avoided in practice where the presence of noise measurements is unavoidable. Indeed, in such a case and according to (17), high values of θ give rise to a high bound for the estimation error since this bound is of the order of θ^{q-1}. Thus, the choice of θ is a compromise between fast convergence and sensitivity to noise.

2.2 A technical lemma

In what follows, a technical lemma together with its proof are given. This lemma will be used to establish the main result of the paper in the next section.

Lemma 2.1 *Consider a differentiable function* $v : t \in I\!R^+ \mapsto v(t) \in I\!R^+$ *satisfying the following inequality:*

$$\dot{v}(t) \leq -av(t) + b\int_{t_k}^{t} v(s)ds + p(t) \quad \forall t \in [t_k, t_{k+1}[\tag{18}$$

with $k \in I\!N$, $t_0 \geq 0$ *where* $0 < \tau_m \leq \tau_k = t_{k+1} - t_k \leq \tau_M < +\infty$, $p(t) : I\!R^+ \to I\!R$ *is an essentially bounded function with* $c = \sup_{t\geq 0} Ess\ p(t)$ *and* a *and* b *are positive reals satisfying* $\frac{b\tau_M}{a} < 1$. *Then, the function* v *satisfies*

$$v(t) \leq e^{-\eta(t-t_0)}v(t_0) + c\tau_M\frac{2-e^{-\eta\tau_m}}{1-e^{-\eta\tau_m}}$$
$$\text{with} \quad 0 < \eta = (a - b\tau_M)\, e^{-a\tau_M} \tag{19}$$

Proof of lemma 2.1. We shall first prove that $v(t) \leq v(t_k) + c(t-t_k) \quad \forall t \in [t_k, t_{k+1}[$ and use this property to establish the key inequality (19). By integrating (18) from t_k to t, we obtain

$$\begin{aligned} v(t) &\leq v(t_k) - a\int_{t_k}^{t} v(s)ds + b\int_{t_k}^{t}\int_{t_k}^{s} v(\nu)d\nu ds + c(t-t_k) \\ &\leq v(t_k) + (b\tau_M - a)\int_{t_k}^{t} v(s)ds + c(t-t_k) \end{aligned} \tag{20}$$

And since $b\tau_M - a < 0$, the last inequality (20) becomes

$$v(t) \ \leq\ v(t_k) + c(t-t_k) \tag{21}$$

Now, we shall establish the inequality (19) using the property (21). Indeed, inequality (18) becomes

$$\begin{aligned} \dot{v}(t) &\leq -av(t) + b\int_{t_k}^{t} (v(t_k) + c(s-t_k))\, ds + p(t) \\ &\leq -av(t) + b\tau_M\, (v(t_k) + c(t-t_k)) + p(t) \end{aligned} \tag{22}$$

Using the comparison lemma and the fact that $b\tau_M < a$, one gets

$$\begin{aligned} v(t) &\leq e^{-a(t-t_k)}v(t_k) + \frac{b\tau_M v(t_k) + c}{a}\left(1 - e^{-a(t-t_k)}\right) \\ &\quad + ca\int_{t_k}^{t}(s-t_k)e^{-a(t-s)}ds \end{aligned} \tag{23}$$

Now, using an integration by part, one can show that

$$a\int_{t_k}^{t}(s-t_k)e^{-a(t-s)}ds = (t-t_k) - \frac{1-e^{-a(t-t_k)}}{a} \tag{24}$$

And substituting (24) in (23), one gets

$$\begin{aligned} v(t) \leq&\ e^{-a(t-t_k)}v(t_k) + \frac{b\tau_M v(t_k) + c}{a}\left(1 - e^{-a(t-t_k)}\right) \\ &+ c((t-t_k) - \frac{1-e^{-a(t-t_k)}}{a}) = g(t)v(t_k) + c(t-t_k) \end{aligned} \tag{25}$$

where $g(t) \triangleq e^{-a(t-t_k)}\,(1 - b\tau_M/a) + b\tau_M/a$.
Let us show that $g(t) \leq e^{-\eta(t-t_k)}$ where η is given as in (19). To this end, it suffices to show that $\delta(t) = \left(g(t) - e^{-\eta(t-t_k)}\right) \leq 0$ for all $t \geq t_k$. This can be done by simply showing that $\dot{\delta}(t) \leq 0$ since one can easily check that $\delta(t_k) = 0$. In fact, this is actually the case since

$$\begin{aligned} \dot{\delta}(t) &= \dot{g}(t) + \eta e^{-\eta(t-t_k)} = -ae^{-a(t-t_k)}(1 - \frac{b\tau_M}{a}) + \eta e^{-\eta(t-t_k)} \\ &\leq -e^{-a\tau_M}(a - b\tau_M) + \eta = 0 \end{aligned} \tag{26}$$

The last equality results from the expression of η given by (19). Hence, inequality (25) becomes

$$v(t) \leq e^{-\eta(t-t_k)}v(t_k) + c(t-t_k), \ \forall t \in [t_k, t_{k+1}[, \ k \in I\!N \tag{27}$$

Iterating inequality (27), one can show that

$$\begin{aligned} v(t_k) \leq&\ e^{-\eta(t_k-t_0)}v(t_0) + c\left(\tau_{k-1} + \tau_{k-2}e^{-\eta\tau_{k-1}}\right. \\ &\left. + \tau_{k-3}e^{-\eta(\tau_{k-1}+\tau_{k-2})} + \ldots + \tau_0 e^{-\eta(\tau_{k-1}+\ldots+\tau_1)}\right) \end{aligned} \tag{28}$$

And using (28), inequality (27) becomes

$$\begin{aligned} v(t) &\leq e^{-\eta(t-t_0)}v(t_0) + c(t-t_k) \\ &\quad + ce^{-\eta(t-t_k)}(\tau_{k-1} + \tau_{k-2}e^{-\eta\tau_{k-1}} \\ &\quad + \tau_{k-3}e^{-\eta(\tau_{k-1}+\tau_{k-2})} + \ldots + \tau_0 e^{-\eta(\tau_{k-1}+\ldots+\tau_1)}) \\ &\leq e^{-\eta(t-t_0)}v(t_0) + c\tau_M(1 + \sum_{j=0}^{k-1} e^{-j\eta\tau_m}) \\ &\leq e^{-\eta(t-t_0)}v(t_0) + c\tau_M\frac{2-e^{-\eta\tau_m}}{1-e^{-\eta\tau_m}} \end{aligned}$$

This ends the proof of the lemma.

3 Design of the continuous-discrete time observer

Before giving the equations of the discrete-continuous time observer, we need the following additional hypothesis on the boundedness of the noise samples $w(t_k)$:
A5. For all t_k, the samples $w(t_k)$ are bounded by δ_w where δ_w is the essential bound given by Assumptions A4.
Now, let us consider the following impulsive system

$$\begin{aligned} \dot{\hat{x}}(t) &= A\hat{x}(t) + \varphi(u(t), \hat{x}(t)) \\ &\quad - \theta\Delta_\theta^{-1}Ke^{-\theta k_1(t-t_k)}(C\hat{x}(t_k) - y(t_k)), t \in [t_k,\ t_{k+1}[\end{aligned} \tag{29}$$

where $\hat{x} = \left(\hat{x}^{1T}\ \ldots\ \hat{x}^{qT}\right)^T$, $K = (k_1 I_p\ \ldots\ k_q I_p)^T$ is the gain matrix where the k_i's, $i = 1, \ldots, q$ are chosen such that the matrix $\bar{A} \triangleq A - KC$ is Hurwitz and Δ_θ is the (bloc) diagonal matrix defined in (7) with $\theta \geq 1$. The following result shows that this impulsive system is a continuous-discrete time observer for system (1).

Theorem 3.1 *Consider the system (1)-(2) subject to Assumption* **A1** *to* **A5**. *Then,* $\forall \rho > 0$; $\exists \theta_0 > 0$; $\forall \theta \geq \theta_0$; $\forall u$ *s.t.* $\|u\|_\infty \leq \rho$; *there exist positive constants* $\chi_\theta > 0$ and $\eta_\theta(\tau_M) > 0$ *such that if the upper bound of the sampling partition diameter* τ_M *is chosen such that* $\tau_M < \chi_\theta$, *then* *for every $\hat{x}(0) \in \mathbb{R}^n$, we have:*

$$\|\hat{x}(t) - x(t)\| \leq \sigma\theta^{q-1}e^{-\eta_\theta(\tau_M)t}\|\hat{x}(0) - x(0)\| + \sigma\tau_M \frac{2-e^{-\eta_\theta(\tau_M)\tau_m}}{1-e^{-\eta_\theta(\tau_M)\tau_m}} \left(\delta_\varepsilon/\theta + \theta^{q-1}\|K\| \left(2 - e^{-k_1\theta\tau_M}\right)\delta_w\right)$$

where x is the unknown trajectory of (1) associated to the input u, $\hat{x}$ is any trajectory of system (29) associated to (u, y), θ_0 is that of theorem 2.1, τ_m and τ_M are defined in (4) with

$$\eta_\theta(\tau_M) = a_\theta \left(1 - \frac{\tau_M}{\chi_\theta}\right) e^{-a_\theta\tau_M}$$
$$\chi_\theta = \frac{\mu}{2(L+\theta)\sigma\|K\|\lambda_M},\ a_\theta = \frac{\mu\theta}{2\lambda_M}$$

Proof of Theorem 3.1: Let $\tilde{x}(t) = \hat{x}(t) - x(t)$ be the observation error, it can be easily checked that

$$\dot{\tilde{x}}(t) = A\tilde{x} + \Phi(u, \hat{x}, x) - \theta\Delta_\theta^{-1}Ke^{-\theta k_1(t-t_k)}C\tilde{x}(t_k) - B\varepsilon(t) + \theta\Delta_\theta^{-1}Ke^{-\theta k_1(t-t_k)}w(t_k)$$

where $\Phi(u, \hat{x}, x) = \varphi(u, \hat{x}) - \varphi(u, x)$. Setting $\bar{x} = \Delta_\theta\tilde{x}$ and using the identities (9) allow to get:

$$\dot{\bar{x}} = \theta A\bar{x} + \Delta_\theta\Phi(u, \hat{x}, x) - \theta Ke^{-\theta k_1(t-t_k)}C\bar{x}(t_k) - \frac{1}{\theta^{q-1}}B\varepsilon(t) + \theta Ke^{-\theta k_1(t-t_k)}w(t_k) \tag{30}$$

Moreover, adding and subtracting the term $\theta KC\bar{x}$ in the last equation yields

$$\begin{aligned}\dot{\bar{x}} &= \theta\left(A - KC\right)\bar{x} + \Delta_\theta\Phi(u, \hat{x}, x) + \theta K(C\bar{x} - e^{-\theta k_1(t-t_k)}C\bar{x}(t_k)) \\ &\quad - B\varepsilon(t)/\theta^{q-1} + \theta Ke^{-\theta k_1(t-t_k)}w(t_k) \\ &= \theta\bar{A}\bar{x} + \Delta_\theta\Phi(u, \hat{x}, x) + \theta Kz - B\varepsilon(t)/\theta^{q-1} + \theta Ke^{-\theta k_1(t-t_k)}w(t_k)\end{aligned}$$

where $z(t) = C\bar{x}(t) - e^{-\theta k_1(t-t_k)}C\bar{x}(t_k) = \bar{x}^1(t) - e^{-\theta k_1(t-t_k)}\bar{x}^1(t_k)$. Notice that $z(t_k) = 0$ and according to (30), the time derivative of z can be written as follows

$$\begin{aligned}\dot{z}(t) &= \dot{\bar{x}}^1(t) + k_1\theta e^{-\theta k_1(t-t_k)}\bar{x}^1(t_k) \\ &= \theta\bar{x}^2 + \Phi^1(u, \hat{x}^1, x^1) + \theta k_1 e^{-k_1\theta(t-t_k)}w(t_k)\end{aligned} \tag{31}$$

where $\Phi^1(u, \hat{x}^1, x^1) = \varphi^1(u, \hat{x}^1) - \varphi^1(u, x^1)$.
Now, let us consider the following candidate quadratic Lyapunov function: $V(\bar{x}) = \bar{x}^T P\bar{x}$ where P is defined as in (8). Proceeding as in the continuous-time output case, one can show that

$$\begin{aligned}\dot{V}(\bar{x}) &= 2\bar{x}^T(t)P\left(\theta\bar{A}\bar{x} + \Delta_\theta\Phi(u, \hat{x}, x) + \theta Kz\right) \\ &\quad -2\bar{x}^T(t)PB\varepsilon(t)/\theta^{q-1} + 2\theta\bar{x}^T(t)PKe^{-\theta k_1(t-t_k)}w(t_k) \\ &\leq -(2\mu\theta - 2L\sqrt{n}\lambda_M)\|\bar{x}\|^2 + 2\theta\bar{x}^T PKz \\ &\quad -2\bar{x}^T(t)PB\varepsilon(t)/\theta^{q-1} + 2\theta\bar{x}^T(t)PKe^{-\theta k_1(t-t_k)}w(t_k)\end{aligned} \tag{32}$$

Choosing θ as in (15), the last inequality (32) becomes

$$\dot{V}(\bar{x}) \leq -\frac{\mu\theta}{\lambda_M}V(\bar{x}) + 2\theta\sqrt{\lambda_M}\|K\|\|z(t)\|\sqrt{V(\bar{x})} + 2\sqrt{\lambda_M}\left(\frac{\|\varepsilon(t)\|}{\theta^{q-1}} + \theta\|K\|\|w(t_k)\|\right)\sqrt{V(\bar{x})}$$

Furthermore, integrating equation (31) from t_k to t while using the fact that $z(t_k) = 0$ yields

$$z(t) = \int_{t_k}^t \left(\theta\bar{x}^2(s) + \Phi^1(u(s), \hat{x}^1(s), x^1(s))\right) ds + \left(1 - e^{-k_1\theta(t-t_k)}\right) w(t_k)$$

Bearing in mind that $\Phi^1(u, \hat{x}^1, x^1) = \varphi^1(u, \hat{x}^1) - \varphi^1(u, x^1)$, one gets

$$\|z(t)\| \leq (\theta + L)\int_{t_k}^t \|\bar{x}(s)\|ds + \left(1 - e^{-k_1\theta(t-t_k)}\right)\delta_w \leq ((\theta + L)/\sqrt{\lambda_m})\int_{t_k}^t \sqrt{V(\bar{x}(s))}ds + \left(1 - e^{-k_1\theta\tau_M}\right)\delta_w$$

Combining the above inequalities, one obtains

$$\begin{aligned}\dot{V}(\bar{x}(t)) &\leq -\frac{\mu\theta}{\lambda_M}V(\bar{x}(t)) \\ &\quad + 2\theta\sqrt{\frac{\lambda_M}{\lambda_m}}\|K\|(\theta + L)\sqrt{V(\bar{x}(t))}\int_{t_k}^t \sqrt{V(\bar{x}(s))}ds \\ &\quad + 2\sqrt{\lambda_M}\left(\frac{\|\varepsilon(t)\|}{\theta^{q-1}} + \theta\|K\|\left(2 - e^{-k_1\theta\tau_M}\right)\delta_w\right)\sqrt{V(\bar{x})}\end{aligned}$$

or equivalently

$$\begin{aligned}\frac{d}{dt}\sqrt{V(\bar{x}(t))} &\leq -\frac{\mu\theta}{2\lambda_M}\sqrt{V(\bar{x}(t))} \\ &\quad + \theta\sigma\|K\|(L + \theta)\int_{t_k}^t \sqrt{V(\bar{x}(s))}ds \\ &\quad + \sqrt{\lambda_M}\left(\frac{\|\varepsilon(t)\|}{\theta^{q-1}} + \theta\|K\|\left(2 - e^{-k_1\theta\tau_M}\right)\delta_w\right)\end{aligned}$$

where $\sigma = \sqrt{\lambda_M/\lambda_m}$ is the conditioning number of P. Finally, let

$$a_\theta = \mu\theta/(2\lambda_M),\ b_\theta = \theta\sigma\|K\|(L + \theta) \ \text{ and}$$
$$p_\theta(t) = \sqrt{\lambda_M}\left(\frac{\|\varepsilon(t)\|}{\theta^{q-1}} + \theta\|K\|\left(2 - e^{-k_1\theta\tau_M}\right)\delta_w\right) \tag{33}$$

and assume that the upper diameter of the sampling partition $\tau_M$satisfies the following condition

$$\tau_M < \frac{a_\theta}{b_\theta} = \frac{\mu}{2(L + \theta)\sigma\|K\|\lambda_M} \triangleq \chi_\theta \tag{34}$$

Then, according to Lemma 2.1, one has

$$\sqrt{V(\bar{x}(t))} \leq e^{-\eta_\theta t}\sqrt{V(\bar{x}(0))} + c_\theta\tau_M\frac{2 - e^{-\eta_\theta\tau_m}}{1 - e^{-\eta_\theta\tau_m}} \tag{35}$$

where

$$c_\theta = \sup_{t\geq 0} Ess\ p_\theta(t) = \sqrt{\lambda_M}\left(\frac{\delta_\varepsilon}{\theta^{q-1}} + \theta\|K\|\left(2 - e^{-k_1\theta\tau_M}\right)\delta_w\right)$$
$$\text{and}\ \ \eta_\theta(\tau_M) = \left(a_\theta - b_\theta\tau_M\right)e^{-a_\theta\tau_M} \tag{36}$$

Coming back to the original coordinates of the observation error $\tilde{x}$ and proceeding as in the continuous measurements case, we get

$$\|\tilde{x}(t)\| \leq \sigma\theta^{q-1}e^{-\eta_\theta(\tau_M)t}\|\tilde{x}(0)\| + \frac{\theta^{q-1}c_\theta\tau_M}{\sqrt{\lambda_m}}\frac{2 - e^{-\eta_\theta(\tau_M)\tau_m}}{\left(1 - e^{-\eta_\theta(\tau_M)\tau_m}\right)} \tag{37}$$

Substituting in the above inequality c_θ by its expression (33) leads to

$$\|\tilde{x}(t)\| \leq \sigma\theta^{q-1}e^{-\eta_\theta(\tau_M)t}\|\tilde{x}(0)\| + N_\theta(\tau_m, \tau_M)\left(\delta_\varepsilon/\theta + \theta^{q-1}\|K\|\left(2 - e^{-k_1\theta\tau_M}\right)\delta_w\right) \tag{38}$$

where

$$N_\theta(\tau_m, \tau_M) = \sigma\theta\tau_M\frac{2 - e^{-\eta_\theta(\tau_M)\tau_m}}{1 - e^{-\eta_\theta(\tau_M)\tau_m}} \tag{39}$$

This completes the proof of theorem 3.1.

Remark 3.1 *In order to put forward the relationship between the rate of the exponential decreasing to zero and the ultimate bound of the observation error given by theorems 2.1 and 3.1, we shall consider the case where the sampling period is constant, namely $\tau_M = \tau_m = T_s$, and we shall closely examine the behaviour of the exponential decay rate and the ultimate bound. Indeed, in such a case, the* *constants η_θ and N_θ respectively defined by (36) and (39) can be considered as functions of the sampling period T_s and specify as follows:*

$$\eta_\theta(T_s) \triangleq (a_\theta - b_\theta T_s)\, e^{-a_\theta T_s}$$
$$N_\theta(T_s) \triangleq \sigma\theta T_s \frac{2-e^{-\eta_\theta(T_s)T_s}}{1-e^{-\eta_\theta(T_s)T_s}} = \sigma\theta T_s \left(1+\frac{1}{1-e^{-\eta_\theta(T_s)T_s}}\right) \quad (40)$$

It is easy to check that for all $T_s \geq 0$ satisfying (34), the first derivative of the function $\eta_\theta(T_s)$ with respect to T_s is non positive and therefore η_θ is a decreasing function of T_s. We now shall show that $N_\theta(T_s)$ is a non decreasing function of T_s. To this end, let us show that the derivative of this function with respect to T_s, denoted by $N'_\theta(T_s)$, is positive. Indeed, one has:

$$\begin{aligned}
&\frac{1}{\sigma\theta}N'_\theta(T_s) = 1+\frac{1}{1-e^{-\eta_\theta(T_s)T_s}} \\
&-T_s\frac{T_s\eta'_\theta(T_s)+\eta_\theta(T_s)}{\left(1-e^{-\eta_\theta(T_s)T_s}\right)^2}e^{-\eta_\theta(T_s)T_s} \\
&\geq 1+\frac{1}{1-e^{-\eta_\theta(T_s)T_s}} - \frac{T_s\eta_\theta(T_s)e^{-\eta_\theta(T_s)T_s}}{\left(1-e^{-\eta_\theta(T_s)T_s}\right)^2} \\
&\qquad (since\ \eta'_\theta(T_s) \leq 0) \\
&= +\frac{1}{1-e^{-\eta_\theta(T_s)T_s}} - \frac{1}{1-e^{-\eta_\theta(T_s)T_s}}\left(\frac{T_s\eta_\theta(T_s)e^{-\eta_\theta(T_s)T_s}}{\left(1-e^{-\eta_\theta(T_s)T_s}\right)}\right) \\
&\geq 1 \quad (since\ \frac{T_s\eta_\theta(T_s)e^{-\eta_\theta(T_s)T_s}}{\left(1-e^{-\eta_\theta(T_s)T_s}\right)} \triangleq \frac{\alpha e^{-\alpha}}{(1-e^{-\alpha})} \leq 1\ \forall\alpha \geq 0)
\end{aligned}$$

Now, let us take the limits of these functions when T_s tends to zero. Indeed, one has:

$$\begin{aligned}
&\lim_{T_s\to 0}\eta_\theta(T_s) = a_\theta = \frac{\mu\theta}{2\lambda_M} \\
&\lim_{T_s\to 0}N_\theta(T_s) = \lim_{T_s\to 0}\frac{\sigma\theta T_s}{1-e^{-\eta_\theta(T_s)T_s}} \\
&\qquad = \lim_{T_s\to 0}\frac{\sigma\theta T_s}{\eta_\theta(T_s)T_s} = \frac{\sigma\theta}{a_\theta} = 2\frac{\lambda_M\sigma}{\mu}
\end{aligned}$$

Furthermore, it is clear that the function $T_s \mapsto \left(\delta_\varepsilon/\theta + \theta^{q-1}\|K\|\left(2-e^{-k_1\theta T_s}\right)\delta_w\right)$ is a non decreasing function of T_s with $\lim_{T_s\to 0}\left(\frac{\delta_\varepsilon}{\theta}+\theta^{q-1}\|K\|\left(2-e^{-k_1\theta T_s}\right)\delta_w\right) = \left(\frac{\delta_\varepsilon}{\theta}+\theta^{q-1}\|K\|\delta_w\right)$ So, the results obtained in the sampled output case are in accordance with those derived in the continuous output one: the decreasing to zero of the observation error is inversely proportional to the magnitude of the sampling period while the value of the ultimate bound is proportional to this magnitude. Moreover, when the sampling period tends to zero, the expressions for the decay rate and ultimate bound are identical to those derived in the continuous output case.

The properties of the continuous-discrete time observer (29) are quite similar to those of the purely continuous-time one. Indeed, in the noise free case and in the absence of uncertainties, i.e. $\delta_\varepsilon = \delta_n = 0$, the observation error converges exponentially to zero. If $\delta_\varepsilon \neq 0$ and is finite, the observation error lies in some ball centered at the origin with a radius proportional to δ_ε but it can be made arbitrarily small by choosing θ sufficiently high. However and as in the continuous case, high values of θ are to be avoided in practice where the presence of the noise measurement is unavoidable. According to (17), high values of θ give rise to a high bound for the estimation error since this bound is of the order of θ^{q-1}. Moreover, very high values of θ may not be allowed since they could violate the condition $\tau_M < \chi_\theta$ given by theorem 3.1.

On other aspects, It is worth noticing that the calibration of the continuous-discrete time observer (29) is mainly achieved through the tuning of the observer design parameter θ as in the continuous-time output case. The specification of this design parameter is commonly carried out bearing in mind a suitable compromise between the convergence speed and the noise measurements insensitivity as pointed out in the earlier contributions on high gain observers [13, 9]. This suitable compromise is generally obtained from a trial and error approach since conditions (15) and (34) are too conservative to provide a reasonable specification of the involved design parameters. An admissible value of the design parameter θ can be used to determine the maximum allowable value for the sampling partition diameter according to inequation (34). Nevertheless, it is possible to find a higher value than the theoretical bound using an appropriate trial and error approach. This issue shall be more discussed and illustrated in simulation through a bioreactor where takes place an ethanolic fermentation.

Notice that thorough investigations addressing the challenging performance improvement issue of high gain observers noise sensitivity have been recently carried out in [2, 6, 23].

4 On-line estimation of the reactions rates in bioreactors

The use of state observers for on-line estimation of the reactions rates in bioreactors has been widely discussed in the literature (see for instance [3, 9, 8, 4] and references therein). However, in most contributions, the proposed estimators assumed continuous outputs measurements. Discrete-time estimators have been proposed to handle the usual case where the output measurements are available only at sampling instants. The underlying design is based on a discrete-time model of the bioreactor resulting from a forward Euler discretization of the continuous time model. We shall show here through a fermentation process how the proposed continuous-discrete time observer can be used for the on-line estimation of the kinetic rates from the available samples corresponding to some components concentrations. More specifically, we consider a fermentation dealing with the production of ethanol (product) by *Saccharomyces cerevisiae* (biomass) which grow on sweet sorghum stalk juice containing glucose as carbon source (substrate) [17, 5]. The bioprocess is operating in a continuous mode with a time-varying dilution rate $D(t)$ and a constant input substrate concentration S_{in}. The mathematical dynamical model of the process is:

$$\left\{\begin{aligned}
\dot{X} &= r_1 - DX \\
\dot{S} &= -\frac{1}{y_{X/S}}r_1 - \frac{1}{y_{P/S}}r_2 + D(S_{in}-S) \\
\dot{P} &= r_2 - DP
\end{aligned}\right. \quad (41)$$

where X, S, P are the respective concentrations of biomass, substrate and product, r_1 and r_2 are the reactions rates and $y_{X/S}$ and $y_{P/S}$ are yield coefficients. The reactions rates r_1 and r_2 are generally very complex functions of the operating conditions and the state of the process. The analytical modelling of these functions is often cumbersome and still constitutes the subject of further and intensive investigations. To tackle this problem, these functions are treated as time-varying parameters that need to be estimated using the measurements of some components concentrations.

By adopting such a strategy, bioengineers would not be brought to choose a particular model amongst the several ones described in the literature. Moreover, these estimates, which are interesting for process control, can also be used for basic investigations of the culture under consideration. In this example, we shall suppose that the substrate and product concentrations are measured and their corresponding measurements are available at sampling instants. The reactions rates r_1 and r_2 shall be treated as time-varying kinetic parameters with unknown dynamics and the objective consists in estimating these key parameters from the measured samples of S and P. Such an objective shall be achieved by considering the following system:

$$\begin{cases} \dot{x}^1(t) = Yx^2(t) - Dx^1 + \begin{pmatrix} DS_{in} \\ 0 \end{pmatrix} \\ \dot{x}^2(t) = \varepsilon(t) \\ y(t_k) = x^1(t_k) \end{cases} \tag{42}$$

where $x^1 = \begin{pmatrix} x_1 = S \\ x_2 = P \end{pmatrix}$, $x^2 = \begin{pmatrix} x_3 = r_1 \\ x_4 = r_2 \end{pmatrix}$,
$Y = \begin{pmatrix} -1/y_{X/S} & -1/y_{P/S} \\ 0 & 1 \end{pmatrix}$ is the matrix of yield coefficients and $\varepsilon = \begin{pmatrix} \varepsilon_1 = \dot{r}_1 \\ \varepsilon_2 = \dot{r}_2 \end{pmatrix}$ is an unknown bounded function.
System (42) can be put under the form (1) by considering the following linear change of coordinates:
$\Phi : \begin{pmatrix} x^1 \\ x^2 \end{pmatrix} \longrightarrow z = \begin{pmatrix} z^1 = x^1 \\ z^2 = Yx^2 \end{pmatrix}$. Hence, a continuous-discrete time impulsive observer of the form (29) can be synthesized for the on line-estimation of the reactions rates r_i's. The equations of the observer can be written in the original coordinates, by considering the inverse of the jacobian transformation as follows:

$$\begin{cases} \dot{\hat{x}}^1(t) = Y\hat{x}^2(t) - D\hat{x}^1 + \begin{pmatrix} DS_{in} \\ 0 \end{pmatrix} \\ \qquad - 2\theta e^{-2\theta(t-t_k)}(\hat{x}^1(t_k) - x^1(t_k)) \\ \dot{\hat{x}}^2(t) = -\theta^2 e^{-2\theta(t-t_k)} Y^{-1}(\hat{x}^1(t_k) - x^1(t_k)) \end{cases} \tag{43}$$

Notice that the gain of the observer (29) is specified in this example as $K^1 = 2I_2$ and $K^2 = I_2$ in such a way that the matrix $A - KC$ has all its eigenvalues located at (-1). We shall provide in the next section some simulation results in order to illustrate performance and the main properties of the proposed observer.

4.1 Simulation results

For simulation purposes and in order to generate the pseudo-measurements of S and P, the reactions rates have to be expressed as functions of the components concentrations. The following expressions have been chosen [17, 5]:

$$r_1 = \frac{\mu_{max}XS}{K_{SX}+S}(1 - K_{PX}P), \; r_2 = \frac{q_{max}XS}{K_{SP}+S}(1 - K_{PP}P) \tag{44}$$

where μ_{max}, q_{max}, K_{SX}, K_{SP}, K_{PX} and $K_{PP}$are constant kinetic parameters. The simulation experiments have been performed using the following initial conditions: $S(0) = \hat{S}(0) = 92.45(g/L)$, $P(0) = \hat{P}(0) = 1.37(g/L)$, $X(0) = 0.19(g/L)$, $\hat{r}_1(0) = \hat{r}_2(0) = 0(1/h)$The values of the kinetic parameters are: $\mu_{max} = 0.259(1/h)$, $q_{max} = 1.916(1/h)$, $y_{X/S} = 0.043(g/g)$, $y_{P/S} = 0.424(g/g)$, $K_{SX} = 0.258(g/L), K_{SP} = 0.83(g/L)$, $K_{PX} = 0.007\,(g/L)^{-1}$, $K_{PP} = 0.01\,(g/L)^{-1}$, $S_{in} = 100(g/L)$. The dilution rate varies as a sinusoidal signal as shown in figure 1. Two simulation sets of results shall be presented depending on whether the outputs are corrupted or not by noise measurements.

4.1.1 The noise-free case

Although this ideal situation is not realistic, it is considered to corroborate the theoretical results obtained through the convergence analysis carried in the above sections. Indeed, according to these results, the ultimate bound for the estimation error can be made as small as desired in the case where the output are available in a continuous manner. If these outputs are available at sampling instants only, then the ultimate bound is an increasing function of the sampling period and it tends to the continuous ultimate bound when the sampling period tends to zero. Indeed, we have reported in figure 2 the estimation errors on the reactions rates provided by the continuous-time observer for two values of θ, namely 50 and 10 and it is clear that the estimation errors decrease when θ increases. Similarly, we have compared in figure 3 the estimation errors issued from the continuous time observer with those corresponding to the continuous-discrete time one when the sampling period is very small, namely $T_s = 0.01h$. For each estimation error, the curves corresponding to the purely continuous-time and continuous-discrete time observers are superimposed. This clearly confirms that the continuous-discrete time observer has a similar behaviour as the purely continuous-time one when the sampling period approaches zero. The estimates of the reactions rates provided by the continuous-discrete time observer are compared with their true evolution, issued from the simulation of system (41), are also provided in figure 3. The accuracy of the provided estimates are worth to be emphasized. However, such an accuracy has been obtained by using sufficiently high values of the observer design parameter θ. As mentioned throughout the previous sections, such values give rise to poor performance in the presence of noise measurements. As a result, in the next section which deals with noisy outputs, lower values for θ shall be considered to ensure a good compromise between accuracy and sensitivity to noise measurements. On other aspects, one recall that the expressions of the reactions rates given by equations (44) are ignored by the the observers (6) and (29). These expressions have been considered in order to generate the pseudo-measurements of S and P used by these observers.

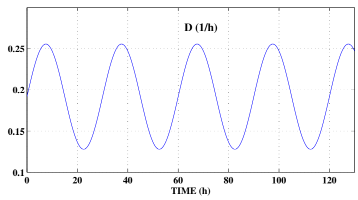

Fig. 1. Time evolution of the dilution rate

4.1.2 The noisy outputs case

In order to simulate practical situations, the measurements of S and P issued from the simulation of system (41)-(44) are corrupted by additive gaussian noises with zero

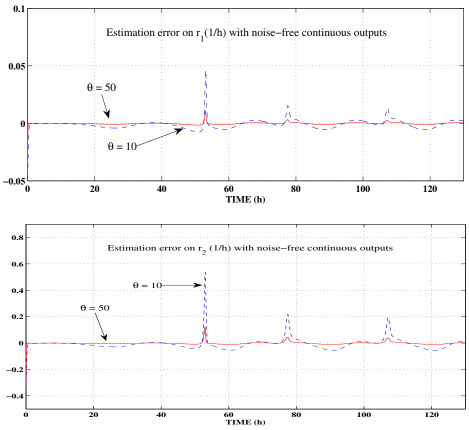

Fig. 2. Estimation of r_1 and r_2 from noise-free continuous outputs

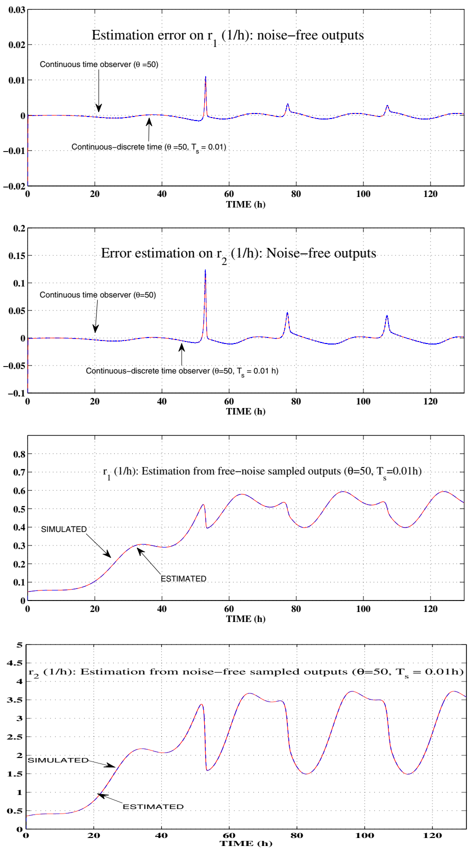

Fig. 3. Estimation of r_1 and r_2 from continuous and sampled outputs

mean value and a variance equal to 0.1 and 0.05, respectively (see figure 4). The simulation study has been performed as follows. First, several simulation experiments have been carried out assuming continuous time output measurements. This allows to obtain a lower bound on the design parameter θ for which the underlying continuous time observer performs well: it ensures a good compromise between a satisfactory tracking of the kinetics unknown dynamics and a well behavior with respect to noise measurements (see figure 5). The value of θ ensuring such a compromise was about 5 which, as expected, is smaller than the values considered in the noise-free case which gave very accurate estimates. Then, the continuous-

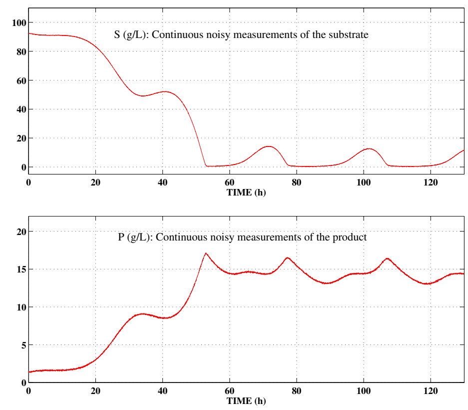

Fig. 4. Continuous noisy measurements of S and P

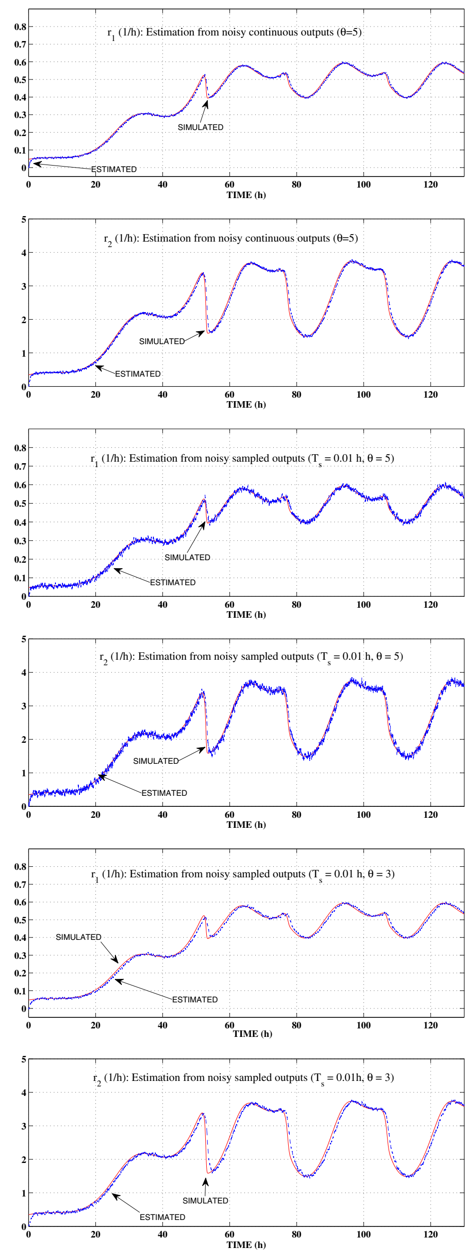

Fig. 5. Estimation of r_1 and r_2 from continuous and sampled noisy outputs ($T_s = 0.01h$)

discrete time observer has been simulated by setting the

design parameter θ to this value while considering a very small constant value for the sampling period e.g. $T_s = 0.01h$. As in the noise free case, the obtained estimates are quite similar, while being somewhat more noisier, to those obtained in the continuous outputs case confirming thereby the theoretical results. Another simulation has been carried out in this case by considering a lower value for the design parameter θ, i.e. $\theta = 3$. The estimates of the reactions rates obtained with this value are smoother than those obtained with $\theta = 5$ but they are less precise since this value does not allow a satisfactory tracking of the reactions unknown dynamics. This explains the phase-shift like behaviour between the provided estimates of the reactions rates and their true values.
In order, to show the behaviour of the continuous-discrete time observers for more higher values of the sampling period, two values of the latter have been considered, $T_s = 0.1h$ and $T_s = 1h$. In each case, the value of the design parameter θ has been chosen by a trial and error approach to get a good compromise between a satisfactory tracking of the kinetics unknown dynamics and a well behavior with respect to noise measurements . Indeed, the value of θ has been set to 3 for $T_s = 0.1h$ and to 2 when $T_s = 1h$. The obtained estimates are given in figure 6 which clearly shows that the continuous-discrete time observer allows a good tracking of the reactions rates while performing well with respect to the noise measurements. Moreover and as expected from the theoretical analysis, the best estimates are obtained with smaller values of the sampling period.

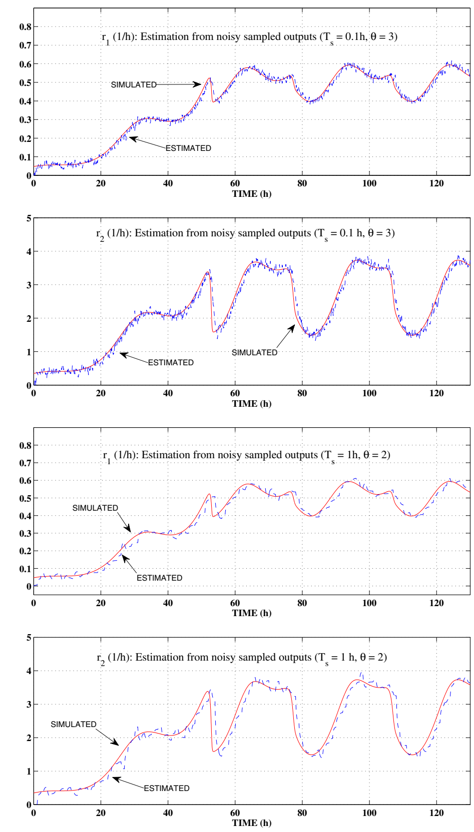

Fig. 6. Estimation of r_1 and r_2 from sampled noisy outputs ($T_s = 0.1h, 1h$)

5 Conclusion

We have derived an impulsive continuous-discrete time high gain observer for a class of nonlinear systems involving some uncertainties and subject to noisy sampled output measurements. The main characteristic of this observer lies in the fact that it provides continuous time estimates of the whole system state from the available output samples. The convergence of the underlying observation error has been established under a well defined condition on the observer, the system parameters (system dimension, Lipschitz constant) and the maximum allowable value of the sampling partition diameter. More specifically, it has been shown that the observation error remains confined in a ball centered at the origin with a radius proportional to the magnitudes of the uncertainties, the measurements noise and the maximum of the sampling partition diameter. The effectiveness of the proposed observers has been illustrated in simulation through an example dealing with an ethanolic fermentation. The obtained results are quite promising to conclude that the proposed observers are able to provide relatively accurate estimates of the reactions rates even in the case of relatively long sampling periods.

References

[1] V. Andrieu and L. Praly. On the existence of Kazantzis-Kravaris / Luenberger observers. *SIAM J. Control and Optimization*, 45:432–456, 2006.

[2] V. Andrieu, L. Praly, and A. Astolfi. High gain observers with updated gain and homogeneous correction terms. *Automatica*, 45:422–428, 2009.

[3] G. Bastin and D. Dochain. *On-line estimation and adaptive control of bioreactors*. Elsevier, Amsterdam, 1990.

[4] H. De Battista, J. Picó, and A. Vignoni. Specific growth rate estimation in (fed-)batch bioreactors using second-order sliding observers. *Journal of Process Control*, 21:1049–1055, 2011.

[5] G. Birol, P. Doruker, B. Kirdar, and K. Ülgen Z.I. Önsan. Mathematical description of ethanol fermentation by immobilised *saccharomyces cerevisiae*. *Process Biochemistry*, 33:763–771, 1998.

[6] N. Boizot, E. Busvelle, and J.P. Gauthier. An adaptive high-gain observer for nonlinear systems. *Automatica*, 46:1483–1488, 2010.

[7] F. Deza, E. Busvelle, J.P. Gauthier, and D. Rakotopara. High gain estimation for nonlinear systems. *Systems & Control Letters*, 18:295–299, 1992.

[8] D. Dochain. State and parameter estimation in chemical and biochemical processes: a tutorial. *Journal of Process Control*, 13:801–818, 2003.

[9] M. Farza, K. Busawon, and H. Hammouri. Simple nonlinear observers for on-line estimation of kinetic rates in bioreactors. *Automatica*, 34(3):301–318, 1998.

[10] M. Farza, M. M'Saad, T. Maatoug, and M. Kamoun. Adaptive observers for nonlinearly parameterized class of nonlinear systems. *Automatica*, 45(10):2292–2299, 2008.

[11] M. Farza, M. M'Saad, and L. Rossignol. Observer design for a class of MIMO nonlinear systems. *Automatica*, 40(1):135–143, 2004.

[12] M. Farza, M. M'Saad, M. Triki, and T. Maatoug. High gain observer for a class of non-triangular systems. *Systems & Control Letters*, 60(1):27–35, 2011.

[13] J.P. Gauthier, H. Hammouri, and S. Othman. A simple observer for nonlinear systems - application to bioreactors. *IEEE Trans. Auto. Control*, 37(6):875–880, 1992.

[14] J.P. Gauthier and I. Kupka. *Deterministic Observation Theory and Applications*. Cambridge University Press, 2001.

[15] H. Hammouri and M. Farza. Nonlinear observers for locally uniformly observable systems. *ESAIM J. on Control, Optimisation and Calculus of Variations*, 9:353–370, 2003.

[16] H. Hammouri, M. Nadri, and R. Mota. Constant gain observer for continuous-discrete time uniformly observable systems. In *Proc. of the the 45th IEEE Conference on Decision and Control*, San Diego, CA, USA, 2006.
[17] H. Jin, R. Liu, and Y. He. Kinetics of batch fermentations for ethanol production with immobilized *saccharomyces cerevisiae* growing on sweet sorghum stalk juice. *Procedia Environmental Sciences*, 12:137–145, 2012.
[18] I. Karafyllis and C. Kravaris. From continuous-time design to sampled-data design of observers. *IEEE Transactions on Automatic Control*, 54(9):2169–2174, 2009.
[19] N. Kazantzis and C. Kravaris. Nonlinear observer design using Lyapunov's auxiliary theorem. *Systems & Control Letters*, 34:241–247, 1998.
[20] H. K. Khalil. *Nonlinear systems.* Printice Hall, third edition, New Jersey, 2003.
[21] A. J. Krener and A. Isidori. Linearization by output injection and nonlinear observers. *Syst. Contr. Lett.*, 3:47–52, 1983.
[22] M. Nadri, H. Hammouri, and R.M. Grajales. Observer design for uniformly observable systems with sampled measurements. *IEEE Transactions on Automatic Control*, 58:757–762, 2013.
[23] M. Oueder, M. Farza, R. Ben Abdennour, and M. M'Saad. A high gain observer with updated gain for a class of MIMO non-triangular systems. *Systems & Control Letters*, 61:298–308, 2012.
[24] T. Raff, M. Kögel, and F. Allgöwer. Observer with sample-and-hold updating for Lipschitz nonlinear systems with nonuniformly sampled measurements. In *Proc. of the American Control Conference*, Washington,USA, 2008.
[25] R. Rajamani. Observers for Lipschitz Nonlinear Systems. *IEEE Transactions on Automatic Control*, 43(3):397–401, 1998.
[26] H. Shim, Y. I. Son, and J. H. Seo. Semi-global observer for multi-output nonlinear systems. *Systems and Control Letters*, 42:233–244, 2001.